A Low-pass Filter with Sharp Transition and Wide Stop-band Designed based on New Metamaterial Transmission Line

L. Peng [1,2], Y. J. Qiu [1], X. Jiang [1], and C. L. Ruan [3]

[1] Guangxi Key Laboratory of Wireless Wideband Communication and Signal Processing
Guilin University of Electronic Technology, Guilin, Guangxi, 541004, China
penglin528@hotmail.com, 524852836@qq.com, jiang_x@guet.edu.cn

[2] Guangxi Experiment Center of Information Science, Guilin, 541004, Guangxi, China
penglin528@hotmail.com

[3] Institute of Applied Physics
University of Electronic Science and Technology of China, Chengdu, Sichuan, 610054, China
rcl@uestc.edu.cn

Abstract ─A low-pass filter (LPF) with sharp and wide stop-band was designed based on new metamaterial transmission line. Its characteristics were investigated, and found to have good low-pass performances with only one cell. The simulated results of the LPF are in good agreements with the measured results. Two measured transmission poles were observed at 1.35 GHz and 2.13 GHz. The measured 3 dB cut-off frequency is 2.38 GHz and the transmission attenuate to -20 dB at 2.62 GHz, thus, a 240 MHz width sharp transition was achieved. The measured attenuation of the stop-band is larger than 25 dB with two transmission zeros at 2.79 GHz and 5.19 GHz. A wide stop-band over 10 GHz was observed. Therefore, the proposed LPF is a good candidate for RF systems.

Index Terms ─ Low-pass filter, metamaterial transmission line, sharp transition, wide stop-band.

I. INTRODUCTION

Compact and high-performance low-pass filters (LPFs) are highly desired in many communication systems as they can be used to suppress undesired harmonics and spurious signals of the mixing products in RF front-ends [1-4]. These designs are based on several design units of defected ground structure (DGS) [1], stepped-impedance resonator (SIR) [2], lumped elements [3], and finite-ground microstrip line [4]. On the other hand, there has been a growing interest for the use of metamaterial transmission lines (TL) in the development of compact microwave components [5-6] and band-pass filters [7-8]. The concept of metamaterial has been successfully utilized to design complementary split ring resonator (CSRR) based band-pass filters (BPF) [9-11] and LPF [12]; however, these filters need multiple units to obtain sharp transition and wide stop-band, which is not suitable for compactness.

In our previous work [13], a novel metamaterial TL with right-hand (RH) property at low and high-frequency bands and left-hand (LH) property at middle-frequency band was analyzed. The TL exhibits low-pass function with/without notches. As discussed in [13], the high RH band can be designed as stop-band through using large grounded capacitance, and the middle LH band can be designed to be impedance mismatch to have a good low-pass response. It is seen that the LH band is the transition between the low-pass and high-stop bands. Thus, narrower LH band means sharper skirt. Besides LH cell is much smaller than the wavelength. Therefore, compact low-pass filter with sharp and wide stop-band can be designed based on such metamaterial TL.

In this work, the designing of LPF based on our previous studied metamaterial TL [13] is proposed. In [13], an implementation of the metamaterial TL was achieved by cross stubs-loaded square DGS and microstrip line-connected equilateral triangle stubs. It is found that the high RH band of the implementation is transmission forbidden due to the large grounded capacitance produced by the equilateral triangle stubs. Its attenuation is up to 30 dB even for a single cell. However, impedance mismatch happens at the upper part of the low RH band and the middle LH band matches well. Thus, a notch was observed for the low-pass response.

To solve this problem, characteristics of the upper part of the low RH band and the middle LH band must be disturbed. Therefore, dimension of the triangle stubs, which correspond to RH characteristics, were adjusted to impedance match the low RH band. Then, parallel

Submitted On: September 2, 2014
Accepted On: August 11, 2016

stubs connected to the cross stubs were utilized to enhanced LH property. The introduced parallel stubs increase the capacitance C_{h1}, the capacitance C_{v2} and the inductance L_{v2}. Thus, LPF's upper edge is greatly decreased, and the transition width between the pass-band and stop-band is improved. Therefore, the proposed design enables a steep attenuation transition from pass- to stop-band and wide stop-band with only one element, while a large number of components are needed in [1-4, 12]. Thereafter, a LPF was designed successfully. As the fabrication of the proposed LPF is based on printed circuit board (PCB) technique, its manufacture is very easy and extremely low cost, as well as facilitating for integrates into integrated circuit (IC).

II. METAMATERIAL LPF DESIGN AND ANALYSIS

A. Metamaterial LPF design

Configuration of the proposed LPF was shown in Fig. 1 (a). The LPF was fabricated on RT/Duroid 5880 substrate with relative permittivity ε_r = 2.2 and thickness 0.508 mm. Two triangle stubs with length of a side L_t were connected to a 50 Ω microstrip line, and one of their peaks locate at the center of the microstrip line. On the other side of the substrate, a square defected pattern was etched in the ground plane with width L. Four cross stubs with width W_1 were placed in the square defected pattern. To enhance LH property, four parallel stubs were introduced by connecting to the four cross stubs, respectively. Then, the LH capacitance C_{h1}, and the capacitance C_{v2} and inductance L_{v2} are increased, which lead to the decreasing of LH frequency and the obtaining of a desired low-pass function. In simulations, the proposed LPF was excited by two wave ports at the ends of the microstrip line. The wave port is used to imitate infinite length of the microstrip line. Typical parameters of the LPF are L = 16 mm, L_t = 10 mm, W_0 = 1.52 mm, W_1 = 1.8 mm, W_2 = 2.15 mm, g = 0.2 mm, and d = 1.5 mm. In many researches, LH properties were obtained by periodic structures, however, according CRLH theory, CRLH property can be achieved by single cell [5, 13]. Then, to obtained compact size, only one cell was used in this design.

The equivalent circuit model of the structure was derived and shown in Fig. 1 (b). The capacitances and inductances are related to certain parts of the LPF structure. The capacitance C_{v2} is owing to the voltage gradients between the triangular stubs and the cross/ parallel stubs. The inductance L_{v2} is generated by the current flowing along the stubs, while the capacitance C_{v3} is engendered by the voltage gradients between the triangular stubs and the ground plane. Then, the shunt resonant tank (Y_2) that forms by C_{v2}, L_{v2} and C_{v3} was obtained. The gap g_0 between the four parallel stubs are used to produce capacitance C_{h1}, while the etched pattern in the ground plane provides inductance L_{h1}. Then, series resonant tank (Z_1) was achieved. The reactance Z_3 (L_{h3}) is due to the current flowing along the microstrip line. Therefore, it is easily understand that the introduction of parallel stubs greatly increase the LH capacitance C_{h1} and the capacitance C_{v2}. The equivalent circuit model is similar to the basic type 1 of the proposed metamaterial TL in [13]. We must point out that this circuit model is rough as some of the distributed effects may not be considered. However, it offers us a way to perceive insight into the structure.

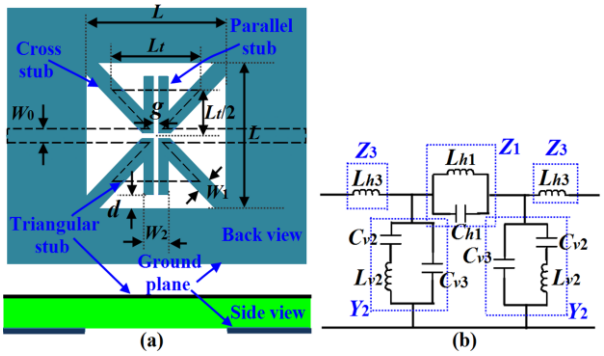

Fig. 1. The proposed LPF: (a) configuration and (b) equivalent-circuit model.

As the *S*-parameters are utilized for *T* type network parameters, effective permittivity and permeability extraction, then, simulated results of the proposed LPF were illustrated in Fig. 2 for further analysis. For comparison, results of a structure without parallel stubs (the inset of Fig. 2) were also demonstrated. It is found from the figure that the proposed LPF exhibits excellent low-pass function, wide stop-band and sharp transition. Its -3 dB upper edge is 2.39 GHz, and its transmission attenuation decrease to -20 dB at 2.65 GHz. Therefore, the transition width is 260 MHz. A wide stop-band with attenuation more than 20 dB was obtained over 10 GHz. The results of the structure without parallel stubs show a -3 dB upper edge at 3.15 GHz. Its transmission attenuation decreases to -20 dB at 3.70 GHz. The transition width is 550 MHz. Though the LPFs with and without parallel stubs have the same size, the one with parallel stubs is much superior in better low-pass impedance matching, lower cut-off frequency and sharper transition between pass-band and stop-band.

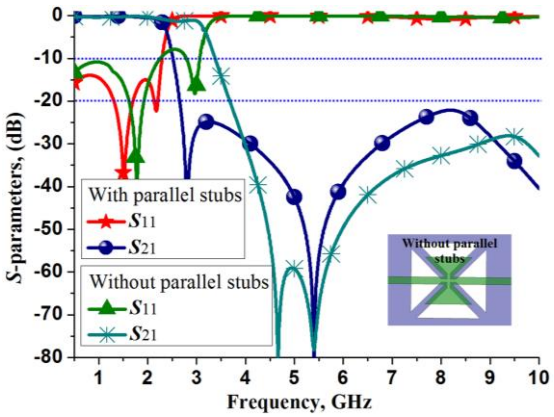

Fig. 2. *S*-parameters with/without stubs.

B. T type network parameters

The derived lumped-circuit model offers us a way to perceive insight into the structure. However, the calculating of the values of the capacitors and inductors is a burdensome and difficult task. Besides, the equivalent circuit model is a rough one with some distribute parameters not considered. Therefore, equivalent *T* type network would be a helpful substitution. Extract the parameters of the equivalent *T* type network is convenient thanks to the microwave network theory and fast developed computer technology. Importantly, *T* type network enable us conveniently and directly cognize the nature of the structure. As the structure is symmetrical, we assumed its *T* type network has horizontal branch Z_1 and vertical branch Z_2 as shown in Fig. 3. Typical *T* type network is derived by solving *ABCD* matrix according to *S* parameters of full wave simulation [14]. Then, we have:

$$Z_1 = (A-1)/C \qquad Z_2 = 1/C. \tag{1}$$

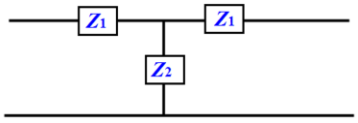

Fig. 3. *T* type network.

The reactance curves of Z_1 and Z_2 of the two LPFs with and without parallel stubs were calculated by formula (1) and illustrated in Fig. 4. Their corresponding S_{21} curves were also plotted in the figure for comparison. It is found that both the structures with/without parallel stubs exhibit LH property (Imag(Z_1) < 0 and Imag(Z_2) > 0) at middle-frequency band and RH property (Imag(Z_1) > 0 and Imag(Z_2) < 0, Imag(Z_2) is close to zero for the high-frequency band) at low- and high-frequency bands. Balanced conditions are met at the transitions between the low-frequency RH band and middle-frequency LH band, while ENG bands [15] (epsilon-negative, Imag(Z_1) > 0 and Imag(Z_2) > 0) were observed between the middle-frequency LH band and the high-frequency RH band. It is found that the introduction of parallel stubs moves the lower edge of LH band from 2.61 GHz to 2.07 GHz and the width of the LH band is reduced from 570 MHz to 380 MHz, consequently, LPF with more compact size and sharper transition is achieved.

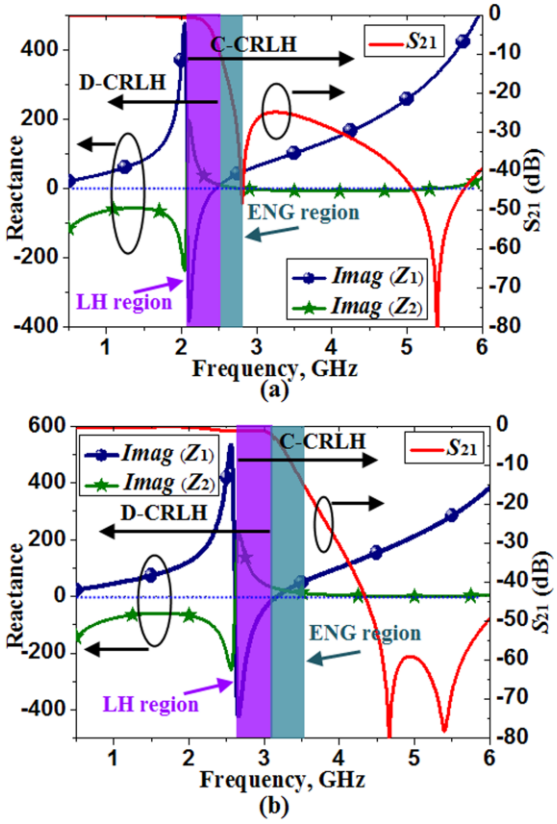

Fig. 4. *T* type parameters and S_{21} parameter: (a) the proposed LPF with parallel stubs, and (b) the LPF without parallel stubs.

C. Effective permittivity and permeability

As the dimension of the unit cell is much less than the operational wavelength, the structure can be characterized by quasi-TEM model and effective medium theory. Thereby, effective permittivity ε_{eff} and effective permeability μ_{eff} will be extracted to further validate our conclusion. An improved Nicolson-Ross-Weir (NRW) approach was adopted for the effective constitutive parameters extraction [16]. First, we list the formula in the following:

$$\mu_{eff} = \frac{2}{jk_0 d}\frac{1-(S_{21}-S_{11})}{1+(S_{21}-S_{11})} \qquad \varepsilon_{eff} = \mu_{eff} + j\frac{2S_{11}}{k_0 d}, \tag{2}$$

where k_0 is the wave number of free space, d is the length of the unit-cell, S_{11} and S_{21} are the scattering parameters. The transmission factor can be described as $\tau = \exp(-jkd)$.

The extracted effective permittivity and permeability

for the structures with/without parallel stubs were illustrated in Fig. 5, and their S_{21} parameters were also presented for comparison. Their effective permittivity and permeability are positive for the low- and high-frequency RH bands, and negative for the middle-frequency LH band. The ENG regions have negative permittivity and positive permeability. The constitutive parameters have good agreement with the *T* type network parameters, then, validity of these extract approaches on our structures were verified.

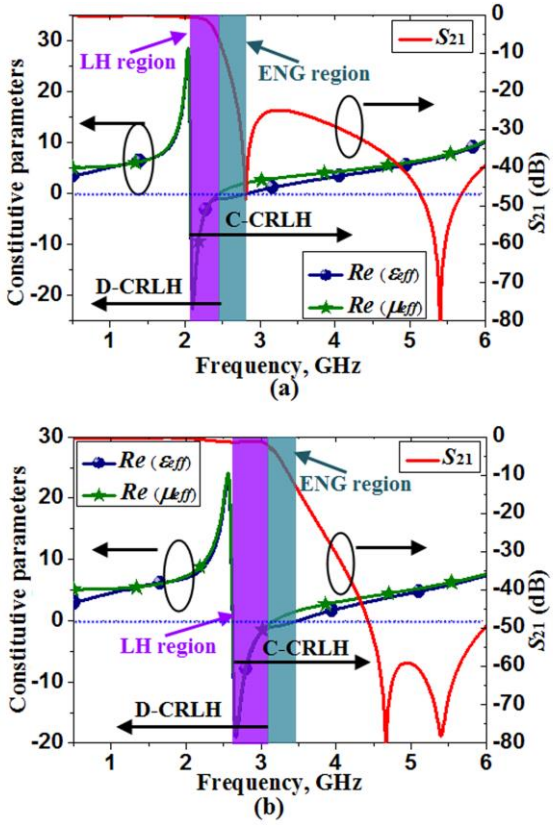

Fig. 5. Constitutive parameters and S_{21} parameter: (a) the proposed LPF with parallel stubs, and (b) the LPF without parallel stubs.

III. RESULTS AND DISCUSSION

We have investigated the LPF by means of equivalent circuit model, *T* type network, and constitutive parameters in Section II. Then, the operational mechanism of the LPF was revealed. To better understand the LPF's characteristics, and utilize it for further design in practical applications, more discussion and results were illustrated in this Section.

A. Parametric study

In Section II A, we found the derived equivalent circuit model elements have certain connection with certain parts of the LPF, therefore, the adjusting of certain parameters of the structure will tune their corresponding capacitances or inductances, consequently LPF performances. Therefore, the proposed LPF with parallel stubs were studied by sweeping its three key parameters (g, d, and L_t) as shown in Fig. 6. The simulated *S*-parameters for the three parameters were demonstrated in Figs. 6 (a), (b) and (c), respectively, while their extracted constitutive parameters were illustrated in Figs. 6 (d), (e) and (f) correspondingly. Note that, when one parameter is changed, others are fixed.

According to the capacitance calculation formulation $C = \varepsilon S/d_0$ of parallel-plate conductors with area S and distance d_0, if the parameter g is increased from 0.2 mm to 0.6 mm, it is equivalent to enlarge the distance d_0. Therefore, the coupling between the parallel stubs is minimized and LH capacitance C_{h1} is decreased. Subsequently, the LH frequency increase as demonstrated in Fig. 6 (d). The ascending of the LH band results in increasing of the cut-off frequency as shown in Fig. 6 (a). While the parameter d increased from 1.5 mm to 5.5 mm, the lengths of the parallel stubs are shortened. Thus, it is equivalent to reduce area S of a parallel-plate, consequently, both the LH capacitance C_{h1} and inductance L_{v2} are decreased. Therefore, both the cut-off frequency and LH band is ascended as exhibited in Figs. 6 (b) and (e). It is found from Figs. 6 (a) and (b) that the decreasing of C_{h1} (LH feature weakened) also leads to a more broadened transition. For example, when g increased from 0.2 mm to 0.6 mm, the width of the transition for -3 dB to -20 dB increased from 260 MHz to 390 MHz, while d increased from 1.5 mm to 5.5 mm, the width transition for -3 dB to -20 dB increased from 260 MHz to 480 MHz. While parameter L_t is increased, the couplings between the triangular stubs and cross/parallel stubs/ground plane are increased. Therefore, both the capacitances C_{v2} and C_{v3} are enhanced. Then, the parameter L_t mainly affects RH characteristics of the proposed LPF. Therefore, the high RH stop-band presents better attenuation and the middle LH band is almost unmoved with L_t increasing as shown in Figs. 6 (c) and (f). However, enhanced RH feature results in difficulty for impedance matching of upper part of low RH band. At last, we can conclude from Fig. 6 that, LH enhancement lead to sharper transition and lower cut-off frequency, while RH enhancement means better high RH stop-band attenuation. However, by considering impedance matching of the pass-band (especially upper part of low RH band), trade-off among impedance matching, transition width and high stop-band must be considered by its LH and RH properties.

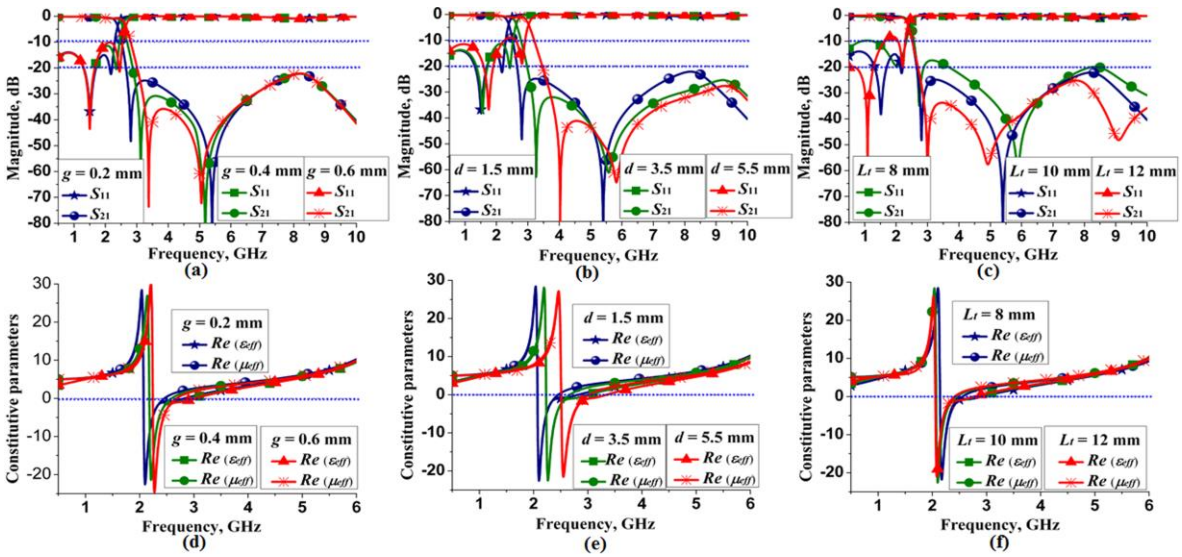

Fig. 6. Frequency responses of the filter: (a) *S*-parameters in terms of g (C_{h1}), (b) *S*-parameters in terms of d (C_{h1} and L_{v2}), (c) *S*-parameters in terms of L_t (C_{v2} and C_{v3}), (d) constitutive parameters in terms of g (C_{h1}), (e) constitutive parameters in terms of d (C_{h1} and L_{v2}), and (f) constitutive parameters in terms of L_t (C_{v2} and C_{v3}).

B. Fabrication and measurement

To further validate the properties of the proposed LPF, it was fabricated as illustrated in Fig. 7. Based on printed circuit board (PCB) technique, the manufacture of the proposed LPF is very easy and extremely low cost, as well as facilitating for integrates into integrated circuit (IC). Two SMA connectors were soldered at the ends of the microstrip fed line for measurement as presented in the figure. Note that, the measurements were performed by an Agilent E5071C ENA series network analyzer with the highest measurable frequency at 8.5 GHz. The simulated and measured *S*-parameters of the proposed LPF are demonstrated in Fig. 8 with good agreements between them observed. The measured 3 dB cut-off frequency is 2.38 GHz with two transmission poles at 1.35 GHz and 2.13 GHz, and two transmission zeros at 2.79 GHz and 5.19 GHz. The transmission attenuation decreased to -20 dB at 2.62 GHz. Therefore, the measured transition width is 240 MHz. Besides, the measured attenuation of the stop-band is larger than 25 dB.

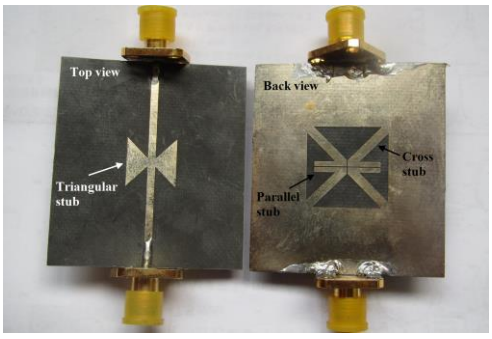

Fig. 7. Photograph of the proposed LPF.

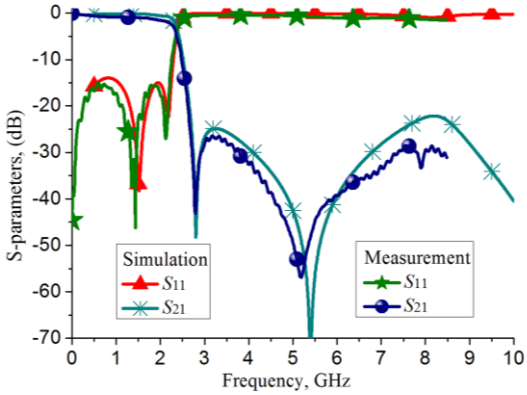

Fig. 8. Simulated and measured *S*-parameters.

IV. CONCLUSION

This paper provides a new approach for LPF designing by applying metamaterial TL technology. Equivalent circuit model of the proposed LPF was derived, and comparison of LPFs with/without parallel stubs was conducted by *S*-parameters, *T* type network parameters and constitutive parameters. Parametric study was performed to reveal the relations between LH/RH characteristics and LPF performances (*S* parameters). Research found the effects of LH and RH features on the cut-off frequency, transition width and high-stop band, which in turn could be used to guide the designing of LPF. The proposed LPF has sharp transition and wide stop-band that turn out to be good candidate for RF front-end circuits.

ACKNOWLEDGMENT

This work is supported in part by National Natural Science Foundation of China (61401110 & 61371056),

in part by Natural Science Foundation of Guangxi (2015GXNSFBA139244), in part by Dean Project of Guangxi Key Laboratory of Wireless Wideband Communication and Signal Processing (GXKL06160109), in part by Guangxi Experiment Center of Information Science (YB1405), and in part by Program for Innovative Research Team of GUET.

REFERENCES

[1] M. A. Aziz, A. M. E. Safwat, F. Podevin, and A. Vilcot, "Coplanar waveguide filters based on multibehavior etched-ground stubs," *IEEE Trans. Comp. Packaging Tech.*, vol. 32, no. 4, pp. 816-824, 2009.

[2] L. Wang, H. C. Yang, and Y. Li, "Design of compact microstrip low-pass filter with ultra-wide stopband using SIRs," *Progress Electromag. Res. Lett.*, vol. 18, pp. 179-186, 2010.

[3] D. Kaddour, E. Pistono, J. Duchamp, J. D. Arnould, H. Eusèbe, P. Ferrari, and R. G. Harrison, "A compact and selective low-pass filter with reduced spurious responses, based on CPW tapered periodic structures," *IEEE Trans. Microw. Theory Tech.*, vol. 54, no. 6, pp. 2367-2375, 2006.

[4] S. Sun and L. Zhu, "Stopband-enhanced and size-miniaturized low-pass filters using high-impedance property of offset finite-ground microstrip line," *IEEE Trans. Microw. Theory Tech.*, vol. 53, no. 9, pp. 2844-2850, 2005.

[5] C. Caloz and T. Itho, *Electromagnetic Metamaterials: Transmission line Theory and Microwave Applications (The Engineering Approach)*. Wiley & Sons, Hoboken, New Jersey, 2006.

[6] R. Marques, F. Martin, and M. Sorolla, *Metamaterials with Negative Parameters: Theory, Design, and Microwave Applications*. John Wiley & Sons, New York, 2008.

[7] M. Oliaei, M. Tayarani, and M. Karami, "Compact microstrip bandpass filter improved by DMS and ring resonator," *Progress Electromag. Res. Lett.*, vol. 45, pp. 7-12, 2014.

[8] M. Gil, J. Bonache, and F. Martín, "Metamaterial filters: A review," *Metamaterials*, vol. 2, no. 4, pp. 186-197, 2008.

[9] J. Bonache, F. Martin, J. García-García, I. Gil, R. Marques, and M. Sorolla, "Ultra wide band pass filters (UWBPF) based on complementary split rings resonators," *Microw. Optical Tech. Lett.*, vol. 46, no. 3, pp. 283-286, 2005.

[10] J. Bonache, I. Gil, J. Garcia-Garcia, and F. Martin, "Novel microstrip bandpass filters based on complementary split-ring resonators," *IEEE Trans. Microw. Theory Tech.*, vol. 54, no. 1, pp. 265-271, 2006.

[11] M. Gil, J. Bonache, J. Garcia-Garcia, J. Martel, and F. Martin, "Composite right/left-handed metamaterial transmission lines based on complementary split-rings resonators and their applications to very wideband and compact filter design," *IEEE Trans. Microw. Theory Tech.*, vol. 55, no. 6, pp. 1296-1304, 2007.

[12] A. Ali and Z. Hu, "Negative permittivity meta-material microstrip binomial low-pass filter with sharper cut-off and reduced size," *IET Microw. Antennas & Propag.*, vol. 2, no. 1, pp. 15-18, 2008.

[13] L. Peng and C. L. Ruan, "Design, analysis and implementation of novel metamaterial transmission line with dual composite right/left-handed and conventional composite right/left-handed properties," *IET Microw. Antennas & Propag.*, vol. 6, no. 15, pp. 1687-1695, 2012.

[14] D. M. Pozar, *Microwave Engineerng. 3rd ed*, J. Wiley, Hoboken, N. J., 2005.

[15] A. Alù and N. Engheta, "Pairing an epsilon-negative slab with a mu-negative slab: resonance, tunneling and transparency," *IEEE Trans. Antennas Propagat.*, vol. 51, no. 10, pp. 2558-2571, 2003.

[16] R. W. Ziolkowski, "Design, fabrication, and testing of double negative metamaterials," *IEEE Trans. Antennas Propagat.*, vol. 51, no. 7, pp. 1516-1529, 2003.

Lin Peng was born in Guangxi Province, China, in 1981. He received the B.E. degree in Science and Technology of Electronic Information, Master and Doctor's degree in Radio Physics from University of Electronic Science and Technology of China (UESTC), Chengdu, China, in 2005, 2008 and 2013, respectively. From 2011 to 2013, he was sponsored by the China Scholarship Council (CSC) to study at the University of Houston (UH) as joint Ph.D. student. From 2013, he joined Guilin University of Electronic Technology (GUET), and became an Associate Professor from Jan. 2016.

Peng has published over 20 papers as first and corresponding author. He is also co-author with over 20 papers. In recent years, he is sponsored by several funds, such as Fundamental Research Funds for the Central Universities, National Natural Science Foundation of China, Program for Innovative Research Team of Guilin University of Electronic Technology, and Guangxi Wireless Broadband Communication and Signal Processing Key Laboratory, etc. Peng serves as Reviewer for *IEEE TMTT*, *IEEE MWCL*, *IEEE AWPL*, *ACES*, *EL*, *Wireless Personal Communications*, *Progress*

in Electromagnetics Research, IET Microwave, Antennas & Propagation, and *Journal of Electromagnetic Waves and Applications*.

Peng's research interests include Antenna/Filter design (For example: communication antennas, Zeroth-order resonator (ZOR) antenna, circular-polarized antenna, UWB antenna, Microstrip antenna and WLAN antenna), Electromagnetic bandgap (EBG) structure design and its application in antenna, Composite right/left-handed (CRLH) transmission line and its applications, and Conformal antenna array.

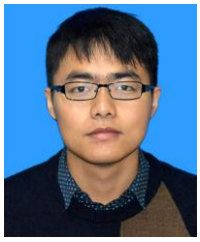

Yu-Jie Qiu was born in Jiangsu Province, China, in 1990. He received the B.E. degree in Communication Engineering from Tongda College of Nanjing University of Posts and Telecommunications, Jiangsu, China, in 2012, and the Master's degree in Electronic and Communication Engineering from Guilin University of Electronic Technology (GUET), Guangxi, China, in 2015. He is currently a Research Assistant at the GUET. His research interests include antennas and metamaterials.

Xing Jiang received the Master's degree in Electromagnetic Field and Microwave Technology from Beijing Institute of Technology (BIT), in 1986. From 2000, she joined Guilin University of Electronic Technology (GUET) as Professor. Jiang has published over 30 papers. She also sponsored by National Natural Science Foundation of China and Natural Science Foundation of Guangxi. Jiang is a Senior Member of China Communications Society, a Member of Chinese Institute of Electronics (CIE). Jiang's research interests include Smart communication system design, Conformal antenna array, and Bio-electromagnetics.

Cheng-Li Ruan received the Ph.D. degree in Electromagnetic Field and Microwave Technology from the University of Electronic Science and Technology of China (UESTC), Chengdu, China, in 1983. From 1985 to 1988, he was an Associate Professor at UESTC. Since 1988, he has been a Professor in the Institute of Applied Physics at UESTC. His current research interests include millimeter wave techniques, electromagnetic scattering, antenna theory, electromagnetic missiles and UWB electromagnetic. He has published over 90 papers on these subjects.

Ruan is a Member of the Chinese Institute of Electronics and the Chinese Electricity Society.